

The interface between the high- $k$  oxide  $\text{LaAlO}_3$  and  $\text{Si}(001)$ Clemens J. Forst,<sup>1,2,3</sup> Dmitri O. Klenov,<sup>4</sup> Susanne Stemmer,<sup>4</sup> Karlheinz Schwarz,<sup>2</sup> and Peter E. Blochl<sup>1</sup><sup>1</sup> Clausthal University of Technology, Institute for Theoretical Physics,  
Leibnizstr.10, D-38678 Clausthal-Zellerfeld, Germany<sup>2</sup> Vienna University of Technology, Institute for Materials Chemistry,  
Getreidemarkt 9/165-TC, A-1060 Vienna, Austria<sup>3</sup> Departments of Nuclear Science and Engineering and Materials Science and Engineering,  
Massachusetts Institute of Technology, Cambridge, Massachusetts 02139, USA and<sup>4</sup> Materials Department, University of California, Santa Barbara, California 93106-5050, USA  
(dated: February 8, 2020)

The structural and electronic properties of the  $\text{LaAlO}_3/\text{Si}(001)$  interface are determined using state-of-the-art electronic structure calculations. The atomic structure differs from previous proposals, but is reminiscent of La adsorption structures on silicon. A phase diagram of the interface stability is calculated as a function of oxygen and Al chemical potentials. We find that an electronically saturated interface is obtained only if dopant atoms segregate to the interface. These findings raise serious doubts whether  $\text{LaAlO}_3$  can be used as an epitaxial gate dielectric.

PACS numbers: 77.55.+f, 68.35.Ct, 71.15Mb, 73.20.-r

One of the key challenges of semiconductor technology in the coming years is the replacement of  $\text{SiO}_2$  as a gate dielectric in microelectronic devices [1]. Due to the downscaling of device dimensions, conventional gate oxides reach a thickness where they lose their insulating properties due to tunneling currents. The replacement of  $\text{SiO}_2$  with high- $k$  oxides, having a larger dielectric constant ( $k$ ), allows to increase the capacitance of the gate stack with a gate oxide of greater physical thickness. However, the growth of high-quality interfaces between Si and high- $k$  oxides remains challenging.

While in a first phase amorphous oxides based on  $\text{ZrO}_2$  or  $\text{HfO}_2$  will be likely employed, industry requires solutions for crystalline oxides with an epitaxial interface to the silicon substrate as soon as possible [1]. The latest edition of the International Roadmap for Semiconductors [1] lists the perovskite  $\text{LaAlO}_3$  (LAO) as a candidate epitaxial oxide. So far, however, there are few demonstrations of atomically well defined interfaces of perovskite oxides grown on silicon, namely  $\text{SrTiO}_3$  (STO) and  $\text{BaTiO}_3$ , as shown by McKee and coworkers [2, 3]. The main reason why STO is not considered as a viable gate dielectric is that its electron injection barrier in the structures prepared so far is too small for transistor applications [4]. Nevertheless, ab-initio calculations [5, 6] provide strong evidence that the band offset can be engineered to meet technological requirements. Besides perovskite oxides, insulator-derived structures are considered promising candidates for epitaxial high- $k$  oxides on silicon [7, 8].

LAO has a dielectric constant of 24 [9], a bandgap of 5.5 eV [10] as compared to 3.2 eV for STO and a large conduction band offset with silicon in its amorphous phase [11]. Thus it seems to provide excellent properties for use as a gate oxide. So far, however, there has been no report of heteroepitaxial growth of LAO on silicon. Experimental studies have been restricted to amorphous

or polycrystalline LAO layers on silicon [11, 12, 13, 14]. Theoretical contributions are limited to a study of a  $(2 \times 1)$  reconstructed interface [15]. Recently, epitaxial growth of silicon with an atomically well defined interface on LAO has been reported [16]. While the reverse growth condition is required for high- $k$  gate oxide applications, a first understanding of the interface was obtained by atomic resolution high-angle annular dark field imaging (HAADF) in scanning transmission electron microscopy (STEM).

Motivated by the work of Klenov et al. [16], we investigated the interface between LAO and silicon with state-of-the-art first-principles calculations. We provide a detailed structural model for the interface and discuss its chemical phase stability with respect to oxygen stoichiometry and doping by Al. We demonstrate that doping is a prerequisite for obtaining an electronically saturated interface as required for its use in a gate stack.

Our results are based on density functional theory calculations [17, 18, 19] using the projector augmented wave method [20, 21] combined with the ab-initio molecular dynamics scheme [22]. All calculations were performed in  $(3 \times 2)$  silicon surface unit cells with a slab thickness of five atomic layers of silicon and 2.5 unit cells (5 atomic layers) of LAO. The LAO layer terminating the  $\text{LaAlO}_3$  slab has been alloyed with 50% Sr to satisfy the electron count at the interface to the vacuum region of around 8 Å [23]. We have used a regular mesh corresponding to 36  $k$ -points per  $(1 \times 1)$  surface unit cell. Further details about the computational procedure can be found in our previous publications in this field [5, 6, 24, 25].

The experimental evidence contained in the scanning transmission electron microscopy images effectively narrows the phase space to be considered in our search for the interface structure. Analysis of these images, shown in Fig. 1, reveals (1) that the La atoms at the interface exhibit a  $(3 \times 1)$  reconstruction, (2) that there are  $2/3 \text{ M L}$

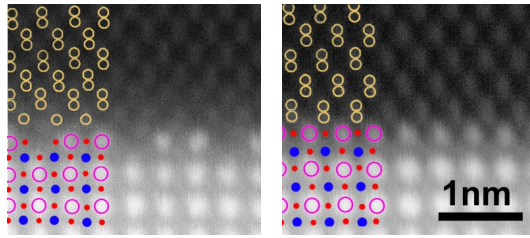


FIG. 1: (Color online) HAADF-STEM images of the interface between LAO and Si [16]. For color coding see Fig. 2.

of La at the interface with double rows of La atoms separated by La-vacancy rows and (3) that the first  $\text{AlO}_2$  layer is a full bulk layer as discussed by Klenov et al. [16]. Other interface configurations, such as one shifted by one half of a unit-cell, were observed as well. They may, however, be related to steps of the LAO substrate.

Despite the high quality of the HAADF-STEM images, certain details of the interface structure cannot be resolved unambiguously. In particular, the details of the Si network at the interface and the oxygen content of the interface cannot be determined from these images. These questions will be addressed in the following. Later we will also investigate the effects of Al doping.

The first question to be addressed is that of the relative orientation of the La-vacancy-rows relative to the silicon dimer rows. The two different choices lead to the structure types denoted A and B as shown in Fig. 2. In structure A the La-vacancy-rows are oriented orthogonal to the Si-dimer rows and in structure B they are parallel. Structure type B reflects the stable surface structures of La adsorbed at silicon at a coverage of  $2/3 \text{ ML}$ , as obtained by first-principles calculations [24]. We furthermore considered interfaces C and D which result from interface B after removal of the silicon dimer rows and isolated silicon atoms, respectively. Removing both silicon dimers and undimerized silicon atoms from structure B yields interface A. Thus we considered a consistent set of trial structures in our search, which had already been identified by Klenov et al. [16].

The stability of the interface structures has to be considered in the light of oxygen stoichiometry, because the interface can exchange oxygen with the oxide by creating or annihilating oxygen vacancies. Following our observation that oxygen attacks the silicon dangling bonds at the STO/Si interface [6], we investigated variants of the interfaces types A–D which are obtained by varying the number of oxidized Si dangling bonds.

For the entire range of oxygen stoichiometries we find that variants of structure type B are more stable than those of interfaces A/C/D by at least  $0.33 \text{ eV}$  per  $(1 \times 1)$  unit cell of the Si surface. In Fig. 3 the energies are shown as function of oxygen chemical potential, which reflects the oxygen partial pressure. Oxidation of the interface starts above an oxygen chemical potential of  $-0.52 \text{ eV}$ .

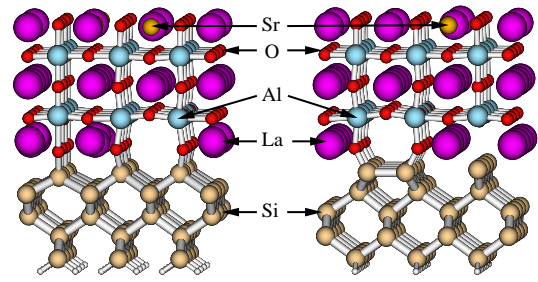


FIG. 2: (Color online) The two limiting cases for the interface structure. Left panel: type A where the dimer rows are orthogonal to the missing La rows; right panel: type B where the dimer rows are parallel to the missing La row. Within each structure type the oxygen content at the interface can vary.

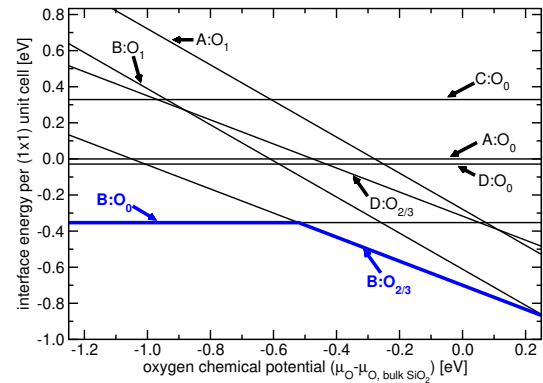


FIG. 3: (Color online) Interface energies per  $(1 \times 1)$  unit cell for the interface types A–D as a function of oxygen chemical potential relative to  $\text{AlO}_2$ . The zero for the oxygen chemical potential is the stability line of Si and  $\text{SiO}_2$ . The labels indicate the interface type and the oxygen content per  $(1 \times 1)$  surface unit cell denoted by  $x$  in  $\text{O}_x$ . Interfaces of type B are stable for the entire range of oxygen chemical potentials.

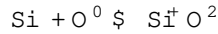
The first oxygen atoms attack the dangling bonds of the Si-dimers, while the isolated silicon atoms of structure type B underneath the La double-row remain vacant. The undimerized silicon atoms resist oxidation up to at a chemical potential of  $+0.27 \text{ eV}$ , which lies beyond the onset of bulk-silicon oxidation.

For use in device applications the interface must be electrically inactive. This implies that the Fermi level is not pinned at the interface. The Fermi level can be pinned either by the interface states located in the band gap of silicon or by the interface being charged so that the charge compensating conduction electrons or holes pin the Fermi level either in the conduction band or the valence band of silicon.

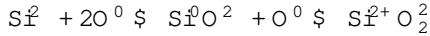
We find that there are no deep interface states in the band gap of silicon, but that all interfaces considered so far are charged. Due to the importance of this finding we discuss the electron count in some detail:

Let us first investigate the oxide: Like STO, LAO crystallizes in the perovskite structure, which consists of alternating layers  $\text{LaO}$  and  $\text{AlO}_2$  stacked in (001) direction. Using the formal charges  $\text{La}^{3+}$ ,  $\text{Al}^{3+}$  and  $\text{O}^{2-}$ , the layers alternate in being positively charged ( $\text{LaO}$ )<sup>+</sup> and negatively charged ( $\text{AlO}_2$ )<sup>-</sup>. This differs from STO where both layers are charge neutral. This seemingly subtle difference does have quite significant implications on the atomic and electronic structure of the interface. In the bulk oxide half of the charge of an  $\text{AlO}_2$  layer is compensated by the  $\text{LaO}$  layer above and the other half by the one below [23]. Thus, an  $\text{AlO}_2$  terminated surface of LAO has a surplus of  $\frac{1}{2}$  electron per (1 × 1) unit cell.

Let us now turn to silicon: Compared to the Si surface, the dangling bond states of the Si atoms at the interface to an oxide are shifted down, almost into the valence band of silicon due to the electrostatic attraction by nearby cations [5]. If the Fermi level is in the band-gap, these orbitals are filled and the silicon atoms have a negative charge. If an oxygen atom binds to silicon, a bonding orbital of mostly oxygen character is formed in the valence band, and an antibonding orbital of mostly silicon character is shifted up into the conduction band, resulting in a (formally) positively charged silicon atom. Thus, the silicon dangling bond is amphoteric in that it changes its formal charge state from negative to positive, while two electrons are transferred to the oxygen atom. For a three-fold coordinated silicon atom we obtain



while for a two-fold coordinated silicon atom we obtain



This explains the somewhat counterintuitive observation that introducing oxygen atoms bound to the silicon atoms at the interface does not affect the net charge of the interface.

Having determined the formal charges of the two half-crystals, we can simply count the remaining charges to determine the net charge of the interface. The  $\text{AlO}_2$  layer contributes a charge of  $\frac{1}{2}$  e per (1 × 1) unit cell. The  $\text{La}_2\text{O}_3$  layer at the interface contributes a charge of +2 e. Since the oxygen stoichiometry of the interface does not change the electron count, we consider the corresponding unoxidized interfaces A and D. Interfaces A and D have one Si-dangling bond per (1 × 1) unit cell while interfaces B and C have  $\frac{4}{3}$  dangling bonds. Since each dangling bond contributes with 1 e, we obtain charges  $q_A = q_D = \frac{1}{2}$  e for interfaces A and D, while interface B and C contribute with  $q_B = q_C = \frac{2}{3}$  e.

To obey the requirement of charge neutrality, this charge must be compensated by the corresponding number of conduction electrons in silicon, which pins the Fermi level at the conduction band for all interfaces considered. Thus none of the interfaces discussed so far is suitable for use in a gate stack.

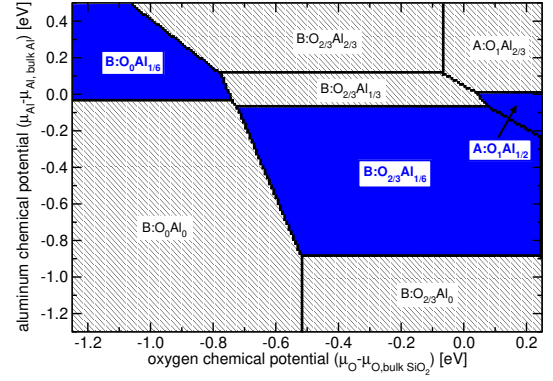


FIG. 4: (Color online) Interface stability as a function of oxygen and aluminum chemical potentials. The interfaces with unpinned Fermi level are shaded in dark (blue). The chemical potentials are plotted relative to the stability line of Si and  $\text{SiO}_2$  as well as that of bulk aluminum. Labels as in Fig. 3

To overcome the above mentioned deficiency, holes have to be introduced. This can be achieved by doping either the oxide or silicon with an acceptor. The only reasonable choice is to replace silicon substitutionally by Al atoms, which act as acceptors.

To reduce the high-dimensional phase space we limited our search to the structure types A and B as the most stable representatives for the two interface charges 1/6 and 1/2. For both structure types we considered structures with the dimer dangling bonds either being unoxidized, denoted as  $\text{A}=\text{B}\text{O}_0$ , or fully oxidized, denoted as  $\text{A}\text{O}_1$  and  $\text{B}\text{O}_{2/3}$ , since these are the oxygen contents that are stable in the thermodynamically accessible range of oxygen chemical potentials (compare Fig. 3). For structure  $\text{B}\text{O}_{2/3}$  we found that replacing the divalent silicon atom by Al is energetically highly unfavorable compared to replacing one of the Si-dimer atoms. Therefore, we limited our search to substitutions of Si-dimer atoms. For the remaining structures we substituted one to four silicon atoms by Al.

The results are composed in the phase diagram shown in Fig. 4. The chemical potentials are given relative to the equilibrium between bulk Si and  $\text{SiO}_2$  for oxygen and to a reservoir of metallic Al on the other hand. Thus only the portion with negative chemical potentials of both, O and Al, is thermodynamically accessible.

To compensate the charge of interface types A and B respectively, substitutional doping with  $\frac{1}{2}$  and  $\frac{1}{6}$  M.L. of Al is required to obtain an electrically inactive interface. Three such regions in the phase diagram are found:  $\text{B}\text{O}_0\text{Al}_{1/6}$ ,  $\text{B}\text{O}_{2/3}\text{Al}_{1/6}$  and  $\text{A}\text{O}_1\text{Al}_{1/2}$ .

While interface B is clearly more favorable for low Al-stoichiometry below  $\frac{1}{6}$  Al per (1 × 1) unit cell, both interface types are nearly isoenergetic for large Al-contents, that is for more than  $\frac{1}{2}$  Al per unit cell. This can be rationalized by the dependence of the formation energy of a substitutional Al in silicon as function of the electron

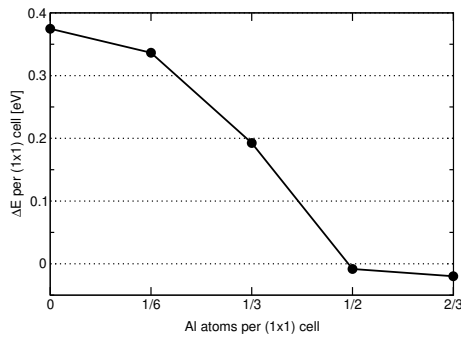


FIG. 5: The energy difference between the interfaces A Si<sub>1</sub> and B Si<sub>2</sub> shown in Fig. 2 as a function of  $N_{A1}$ , the number of substitutional Al atoms at the interface per (1 × 1) unit cell.  $\phi_0$  has been set equal to the coexistence of Si and SiO<sub>2</sub>.

chemical potential. The formation energy depends on the electron chemical potential since  $E^f(\cdot) = E^f(\cdot) - \mu$  for values within the silicon band gap, i.e. for  $\mu_v < \mu < \mu_c$ . Thus it costs less energy to introduce an Al atom, when the Fermi level is pinned at the conduction band than at the valence band. This leads to the step-like shape of the relative energies of structure type A and B as a function of the Al content shown in Fig. 5. If the Fermi levels are equal, to a first approximation, the energy to substitute one Si by an Al atom is identical for both interfaces, explaining the approximately flat behavior for  $N_{A1} < \frac{1}{6}$  and for  $N_{A1} > \frac{1}{2}$ . In the crossover region, that is for  $\frac{1}{6} < N_{A1} < \frac{1}{2}$  the Fermi level for the A-type interface is pinned at the conduction band while that of the B-type interface is pinned at the valence band, resulting in a slope of approximately the silicon band gap versus  $N_{A1}$ . We may speculate that the strong dependence of the segregation energy of Al on the Fermi-level position leads to self-compensation during growth.

Furthermore, Fig. 4 reveals that oxidation of the dangling bonds significantly stabilizes the substitution of Si by Al, since the corresponding phase boundaries are shifted to lower Al chemical potentials when the dangling bonds are oxidized.

In conclusion, we determined the atomic structure and stoichiometry of the LaAlO<sub>3</sub>/Si interface. Without doping, the Fermi level is pinned in the conduction band of silicon, a result that is independent of the oxygen content of the interface. For a technologically viable interface, dopant atoms need to segregate at the interface. A phase diagram for variable oxygen- and aluminum-content is provided. Our results cast doubt that LaAlO<sub>3</sub> can be used as epitaxial gate oxide. Its use depends on the ability to precisely control the aluminum content of the interface which may, however, be facilitated by a self-compensation mechanism.

The authors thank A. Reyes Huamantla for contributions in the initial stage of the project. C.F. acknowledges the support of S. Yip and J. Li. D.K. and S.S. gratefully acknowledge D. Schlom and H. Li for the

LAO/Si samples. This project received funding from the European Commission (project "ET4US"), HLRN, the Austrian Science Fund (project "AURORA"), NSF (CHE-0434567) and SRC.

- 
- [1] International Technology Roadmap for Semiconductors, 2003 Ed. <http://public.itrs.net/>
  - [2] R.A. McKee, F.J. Walker and M.F. Chisholm, Phys. Rev. Lett. 81, 3014 (1998).
  - [3] X. Hu et al., Appl. Phys. Lett. 82, 203 (2002).
  - [4] S.A. Chambers, Y. Liang, Z. Yu, R. Droopad, and J. Ramdani, J. Vac. Sci. Technol. A 19, 934 (2001).
  - [5] C.R. Ashman, C.J. Forst, K. Schwarz and P.E. Blochl, Phys. Rev. B 69, 75309 (2004).
  - [6] C.J. Forst, C.R. Ashman, K. Schwarz and P.E. Blochl, Nature 427, 53 (2004).
  - [7] S. Guha, N.A. Bojarczuk, and V. Narayanan, Appl. Phys. Lett. 80, 766 (2002).
  - [8] J.W. Seo, J. Fompeyrine, A. Guiller, G. Norga, C. Marchiori, H. Siegwart, and J.P. Locquet, Appl. Phys. Lett. 83, 5211 (2003).
  - [9] R. Schwab, R. Spörl, P. Severloh, R. Heidinger, and J. Halbritter, in Applied Superconductivity 1997, Vols 1 and 2 (1997), p. 61.
  - [10] S.G. Lim, S.K. Riventsov, T.N. Jackson, J.H. Haeni, D.G. Schlom, A.M. Balbashov, R. Uecker, P. Reiche, J.L. Freeouf, and G. Lucovsky, J. Appl. Phys. 91, 4500 (2002).
  - [11] L.F. Edge, D.G. Schlom, S.A. Chambers, E. Cicarella, J.L. Freeouf, B. Hollander and J. Schubert, Appl. Phys. Lett. 84, 726 (2004).
  - [12] B.E. Park and H. Ishiwara, Appl. Phys. Lett. 82, 1197 (2003).
  - [13] A.D. Li, Q.Y. Shao, H.Q. Ling, J.B. Cheng, D.W. Wu, Z.G. Liu, N.B. Ming, C.W. Wang, H.W. Zhou and B.Y. Nguyen, Appl. Phys. Lett. 83, 3540 (2003).
  - [14] L.F. Edge, D.G. Schlom, R.T. Brewer, Y.J. Chabal, J.R. Williams, S.A. Chambers, C. Hinkle, G. Lucovsky, Y. Yang, S. Stemmer, M. Copple, B. Hollander and J. Schubert, Appl. Phys. Lett. 84, 4629 (2004).
  - [15] J. Robertson and P.W. Peacock, Mat. Res. Soc. Symp. Proc. 786, 23 (2004), Phys. Stat. Sol. 241, 2236 (2004).
  - [16] Dmitri O.K. Lenov, Daniel G. Schlom, Hao Li and Susanne Stemmer, Jap. J. Appl. Phys. 44, L617 (2005).
  - [17] P. Hohenberg and W. Kohn, Phys. Rev. 136, B864 (1964).
  - [18] W. Kohn and L.J. Sham, Phys. Rev. 140, A1133 (1965).
  - [19] J.P. Perdew, K. Burke, and M. Ernzerhof, Phys. Rev. Lett. 77, 3865 (1996).
  - [20] P.E. Blochl, Phys. Rev. B 50, 17953 (1994).
  - [21] Peter E. Blochl, Clemens J. Forst and Johannes Schimpl, Bull. Mater. Sci. 26, 33 (2003).
  - [22] R. Car and M. Parrinello, Phys. Rev. Lett. 55, 2471 (1985).
  - [23] P.W. Tasker, J. Phys. C 12, 4977 (1979).
  - [24] C.R. Ashman, C.J. Forst, K. Schwarz and P.E. Blochl, Phys. Rev. B 70, 155330 (2004).
  - [25] C.J. Forst, C.R. Ashman, K. Schwarz and P.E. Blochl, Microelectronic Engineering, in press;